社団法人 電子情報通信学会
THE INSTITUTE OF ELECTRONICS,
INFORMATION AND COMMUNICATION ENGINEERS

信学技報
IEICE Technical Report
CAS2011-44,NLP2011-71(2011-10)

複数家庭で構成される電力システムの非線形ダイナミクスと安定性

薄 良彦† 風岡 諒哉† 引原 隆士†

† 京都大学大学院 工学研究科 電気工学専攻
〒615-8510 京都市西京区京都大学桂
E-mail: †susuki@dove.kuee.kyoto-u.ac.jp, ††kazaoka@circuit.kuee.kyoto-u.ac.jp,
†††hikihara@kuee.kyoto-u.ac.jp

あらまし 本報告では複数家庭で構成される電力システムの非線形ダイナミクス及び安定性を検討する．家庭とは，再生可能エネルギーを用いた分散型電源，負荷，電力変換回路などで構成される家屋内の小容量電力システムを意味し，消費側の電力マネージメント技術に関連し近年注目を集めている．本報告では，複数の家庭及び商用電源を配電ネットワークを介して結合したシステムのダイナミクスを数値的に検討し，超臨界ホップ分岐に伴う持続振動が周波数及び有効電力に生起することを指摘する．さらに，上述の分岐及び振動現象に基づいて，分散型電源における入力不確定性の各家庭の有効電力出力への影響を検討する．

キーワード 電力システム，家庭，非線形ダイナミクス，安定性，スマートコミュニティ

Nonlinear dynamics and stability of an electric power system with multiple homes

Yoshihiko SUSUKI†, Ryoya KAZAOKA†, and Takashi HIKIHARA†

† Department of Electrical Engineering, Kyoto University
Katsura, Nishikyo, Kyoto 615-8510 Japan
E-mail: †susuki@dove.kuee.kyoto-u.ac.jp, ††kazaoka@circuit.kuee.kyoto-u.ac.jp,
†††hikihara@kuee.kyoto-u.ac.jp

Abstract We study nonlinear dynamics and stability of an electric power system with multiple homes. The notion of home is a unit of small-scale power system close to consumers that includes own renewable energy source, residential load, and power conversion circuits. An entire power system consists of multiple homes that are interconnected via a distribution network and are connected to the commercial power grid. Numerical simulations allow us to investigate dynamics of the power system, in which supercritical Hopf bifurcation and associated sustained oscillations in frequency and active power are identified. A dynamical effect of uncertainty in a renewable energy source to the active power output of homes is also identified.

Key words electric power system, home, nonlinear dynamics, stability, smart community

1. Introduction

Electrical energy distribution has been traditionally managed by central suppliers. Due to nonlinear dynamics with multiple scales in time and space, this is a very challenging task, especially on the distributed, demand side. Many researchers begin intensive efforts to overcome this challenge by an integration of ideas from information, communication, power, and control technologies. The integration begins at the smallest grid inside the home, then moves to building units, and finally reaches the local area. There are many ongoing research projects on electrical energy distribution [1–3]. Understanding nonlinear dynamics of this complex engineered system is the key enabler to accomplishing the distribution in a stable, resilient, and energy-efficient way [4].

In this report, we present an initial study on nonlinear dynamics and stability of an electric power system with multiple homes. The notion of *home* used here is a unit of small-scale power system close to consumers. The home consists of

multiple power sources, (residential) loads, power conversion circuits, and control systems. Examples of the power sources are photovoltaic (PV) array, micro-cogeneration plant, fuel cell, and large Lithium-Ion battery. An entire power system includes multiple homes that are interconnected via a distribution network and are connected to the commercial power grid. First, we introduce a physical configuration of the power system with multiple homes that we analyze in this report. A key point of this configuration is the technology of bi-directional, single-phase grid-connected inverters that is proposed in [5–7] and termed in [7] as the *synchronous inverter*. This application makes it possible to connect a home with the outside of it, to maintain frequency synchronization, which is a dynamical analogue of synchronous generators, and to enhance stability of the entire power system against a disturbance. We will term the inverter circuit as the *interface circuit*. Second, we develop a mathematical model that represents nonlinear slow dynamics of the power system. The slow dynamics correspond to time responses of frequency and active power in the mid- and long-term regime (order of seconds to hours). Third, we present an example of the dynamics of the system in a realistic setting of parameters. The setting is based on commercial residential buildings and power conditioning systems in Japan. Numerical simulations of the mathematical model allow us to investigate the dynamics, in which supercritical Hopf bifurcation and associated sustained oscillation in frequency and active power are identified. Also we illustrate a dynamical effect of uncertainty in a renewable energy source to the active power output of each home. This report is a summarized version of the conference proceedings [8,9] and focuses on dynamics parts in them.

2. System Configuration and Mathematical Models

In this section, we introduce a configuration of electric power systems with three homes and derive a mathematical model that represents dynamics of the power system. Each home includes a PV generation unit, an in-home dc load, and an interface circuit. Fig. 1 shows a prototype of the power system in which three homes are interconnected via a ladder-type inter-home network. Before modeling in this section, we make the following assumptions:

- Voltage amplitude is regulated at a nominal value.
- Interface circuit is lossless, and its operation is ideal.
- Inter-home distribution network consists of passive elements.
- Every home has the same equipment of the in-home system.
- The commercial power grid is regarded as the infinite bus [10].

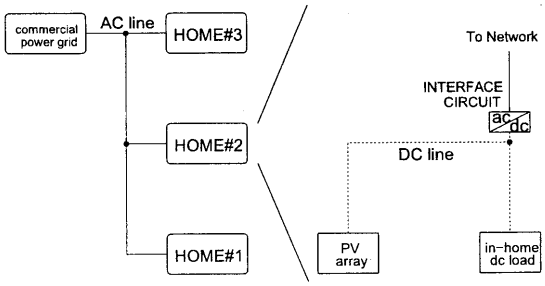

Fig. 1 Configuration of electric power systems with multiple homes. This is a prototype of the power system in which three homes are interconnected via a ladder-type inter-home network. Each home has a simple structure of a photovoltaic (PV) array, an in-home dc load, and an interface circuit.

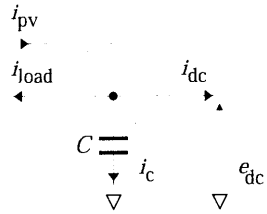

Fig. 2 Current variables defined in the in-home power system. The normalized photovoltaic output current is denoted by i_{pv}, the load input current by i_{load}, the dc current by i_{dc}, and the capacitor current by i_c. The capacitor C is introduced in order to smooth the dc system voltage e_{dc}.

All of the assumptions are reasonable for developing mathematical models of nonlinear slow dynamics in the power system. Table 1 is a list of parameters that we use throughout the report.

Here we provide the basic idea of mathematical modeling for the dynamics of power system. For each component in the homes, we provide a mathematical description of the relationship between the dc system voltage e_{dc} and an output current. We denote by i_{pv}, i_{load}, and i_{dc} the normalized PV output current, load input current, and dc current: see Fig. 2. The normalized capacitor current with constant capacitance C is also denoted by i_c. In Fig. 2, the Kirchhoff's current law gives the following equality: at any moment t,

$$i_{pv}(t) = i_{load}(t) + i_{dc}(t) + i_c(t). \quad (1)$$

The relationship between e_{dc} and i_c is simply the following:

$$C\frac{de_{dc}}{dt} = i_c. \quad (2)$$

2.1 PV Generation Unit

Figure 3 shows the simple circuit model of a PV cell which we use in this report. This circuit model consists of the ideal dc current source i_{ph}, the ideal diode, and the shunt resistance $R_{sh(pv)}$. The parameter i_{ph} is the photoelectronic current produced in the cell. In this model, the following relationship between the cell output current $i_{pv(c)}$ and the

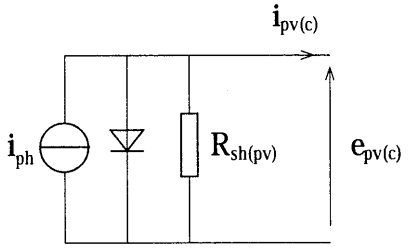

Fig. 3 Simple circuit model of a PV cell. This model consists of the photoelectronic current source $i_{\rm ph}$, the ideal diode, and the shunt resistance $R_{\rm sh(pv)}$.

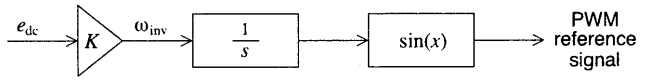

Fig. 4 Block diagram of the Voltage-Controlled Oscillator (VCO) that produces the PWM reference signal [7]. The VCO achieves frequency synchronization between different homes.

cell terminal voltage $e_{\rm pv(c)}$ holds:

$$i_{\rm ph} = I_0 \left\{ \exp\left(\frac{e_{\rm pv(c)}}{V_T}\right) - 1 \right\} + \frac{e_{\rm pv(c)}}{R_{\rm sh(pv)}} + i_{\rm pv(c)}, \qquad (3)$$

where I_0 is the reverse bias saturation current, and V_T is the thermal voltage at temperature T in Kelvin. Let us read $i_{\rm pv}$ as the output current of a PV array that consists of $N_{\rm s}$ cells in series and $N_{\rm p}$ cells in parallel. In this way, $i_{\rm pv}$ is represented as

$$i_{\rm pv} = N_{\rm p} i_{\rm pv(c)} = N_{\rm p} \left[i_{\rm ph} - I_0 \left\{ \exp\left(\frac{e_{\rm dc}}{N_{\rm s} V_T}\right) - 1 \right\} - \frac{e_{\rm dc}}{N_{\rm s} R_{\rm sh(pv)}} \right], \qquad (4)$$

where we used the direct relation $e_{\rm pv(c)} = e_{\rm dc}/N_{\rm s}$ under an additional assumption of the PV array in which each cell has a common value of terminal voltage.

2.2 In-home DC Load

Simply, we consider the in-home load as a constant power load, which is denoted by $p_{\rm load}$. Then the load input current $i_{\rm load}$ is represented as

$$i_{\rm load} = \frac{p_{\rm load}}{e_{\rm dc}}. \qquad (5)$$

2.3 Interface Circuit

Basically, we use the mathematical model of the interface circuit presented in [5,7], but we improve it slightly in order to represent interaction dynamics of multiple homes. Fig. 4 shows the block diagram of the Voltage-Controlled Oscillator (VCO) that produces the PWM reference signal. The mathematical model of the VCO is simply the following:

$$\omega_{\rm inv} = \frac{\omega_0}{E_0} e_{\rm dc} = K(e_{\rm dc} - E_0) + \omega_0, \qquad (6)$$

where ω_0 is the nominal angular frequency, E_0 is the nominal value of $e_{\rm dc}$, and $K := \omega_0/E_0$ is the gain constant for

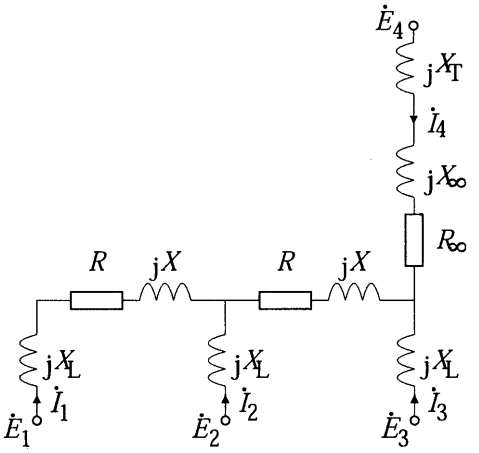

Fig. 5 Inter-home distribution network for the electric power system with three homes. It consists of passive elements that are lumped resistances and reactances. A step-up transformer is introduced at the linkage point between the system and the commercial grid.

frequency regulation. By defining the new variable $\Delta\omega$ as $\omega_{\rm inv} - \omega_0$, we have

$$\Delta\omega = K(e_{\rm dc} - E_0). \qquad (7)$$

Here, by the assumption that the interface circuit is lossless, we have the following equality of active power balance that bridges between the dc and ac systems:

$$e_{\rm dc} i_{\rm dc} = {\rm Re}[\dot{E}\dot{I}^*] =: p, \qquad (8)$$

where we denote by $\dot{E}$ (or $\dot{I}$) the ac output voltage (or current) of the interface circuit in phasor, and the symbol $*$ stands for the conjugate operation of complex variables. The variable δ is termed as the phase angle in literature of power systems engineering [10]. With (1), (2), (7), and (8), we have the following differential equations that represent the time changes of δ and $\Delta\omega$:

$$\left.\begin{aligned} \frac{{\rm d}\delta}{{\rm d}t} &= \Delta\omega, \\ \frac{{\rm d}\Delta\omega}{{\rm d}t} &= \frac{K}{C}\left(i_{\rm pv} + i_{\rm batt} - i_{\rm load} - \frac{p}{e_{\rm dc}}\right), \end{aligned}\right\} \qquad (9)$$

where we recall that $e_{\rm dc}$ is a function of $\Delta\omega$. The term p of the active power output from a single home is derived in the next sub-section.

2.4 Inter-home Distribution Network

Finally, we model the inter-home distribution network and derive the formula of active power output p of a home. Consider the inter-home distribution network with the ladder topology shown in Fig. 5. The parameters R, X, R_∞, X_∞, $R_{\rm L}$, $X_{\rm L}$, and $X_{\rm T}$ are constant and given in Tab. 1. For the network without the linkage reactors ($X_{\rm L}$) and step-up transformer ($X_{\rm T}$), the cutset matrix C, the branch admittance matrix $\mathsf{Y}_{\rm branch}$, and the admittance matrix Y are defined as follows:

$$\left.\begin{aligned} \mathsf{C} &:= \begin{pmatrix} 1 & 0 & 0 \\ -1 & 1 & 0 \\ 0 & -1 & 1 \\ 0 & 0 & -1 \end{pmatrix}, \\ \mathsf{Y}_{\text{branch}} &:= \operatorname{diag}(((R+\mathrm{j}X)^{-1}, (R+\mathrm{j}X)^{-1}, \\ &\quad (R_\infty+\mathrm{j}X_\infty)^{-1})^\top), \\ \mathsf{Y} &= \mathsf{C}\mathsf{Y}_{\text{branch}}\mathsf{C}^\top, \end{aligned}\right\} \quad (10)$$

where $\top$ stands for the transpose operation of vectors and matrices. Here, the relation $\dot{\boldsymbol{I}} = (\mathsf{G}+\mathrm{j}\mathsf{B})\dot{\boldsymbol{E}}$, where $\dot{\boldsymbol{I}} := (\dot{I}_1, \ldots, \dot{I}_4)^\top$ (or $\dot{\boldsymbol{E}} := (\dot{E}_1, \ldots, \dot{E}_4)^\top$) is the output current (or voltage) vector of the three interface circuits and the commercial grid, is used for the derivation of p_k of active output power from home #k ($k = 1, 2, 3$): The two real-valued matrices G and B of the admittance matrix Y are directly calculated as follows:

$$\mathsf{G}+\mathrm{j}\mathsf{B} = (\mathsf{I}_4 + \mathsf{Y}\operatorname{diag}(\dot{\boldsymbol{Z}}_{\text{link}}))^{-1}\mathsf{Y}, \quad (11)$$

where I_4 is the identity matrix of size 4, and $\dot{\boldsymbol{Z}}_{\text{link}}$ the linkage impedance vector given by

$$\dot{\boldsymbol{Z}}_{\text{link}} := \mathrm{j}(X_{\text{L}}, X_{\text{L}}, X_{\text{L}}, X_{\text{T}})^\top. \quad (12)$$

Thus, we have the following expression of the active power output p_k:

$$\begin{aligned} p_k &:= \operatorname{Re}[\dot{E}_k \dot{I}_k^*] \\ &= G_{kk}E_k^2 + \sum_{l=1, l\neq k}^{4} E_k E_l \{G_{kl}\cos(\delta_k - \delta_l) \\ &\quad + B_{kl}\sin(\delta_k - \delta_l)\}, \end{aligned} \quad (13)$$

where G_{kl} (or B_{kl}) stands for the matrix entry of G (or B) in the k-th row and l-th column. The term p_k is a function of phase angles δ_k in all the homes and the infinite bus.

2.5 Full Model

As a result, we have the full model that represents the dynamics of frequency and active power in the three homes: for home #k ($k = 1, 2, 3$),

$$\left.\begin{aligned} \frac{\mathrm{d}\delta_k}{\mathrm{d}t} &= \Delta\omega_k, \\ \frac{\mathrm{d}\Delta\omega_k}{\mathrm{d}t} &= \frac{K}{C}\left(i_{\text{pv},k} - \frac{p_{\text{load},k}}{e_{\text{dc},k}} - \frac{p_k}{e_{\text{dc},k}}\right), \\ e_{\text{dc},k} &= E_0 + \frac{\Delta\omega_k}{K}, \\ i_{\text{pv},k} &= N_{\text{p}}\left[i_{\text{ph},k} - I_0\left\{\exp\left(\frac{e_{\text{dc},k}}{N_{\text{s}}V_T}\right) - 1\right\}\right. \\ &\quad \left. - \frac{e_{\text{dc},k}}{N_{\text{s}}R_{\text{sh(pv)}}}\right], \end{aligned}\right\} \quad (14)$$

where the term p_k of the active power output is presented in (13).

3. Numerical Simulations

In this section, we present a result on numerical simulations of (14). Equation (14) possesses many uncertain parameters that include the injection current $i_{\text{pv},k}$ of the PV array and the load profile $p_{\text{load},k}$. We numerically investigate the dynamics of the system under a change of the parameter of the PV array. The setting of parameters for numerical simulations is given in Tab. 1.

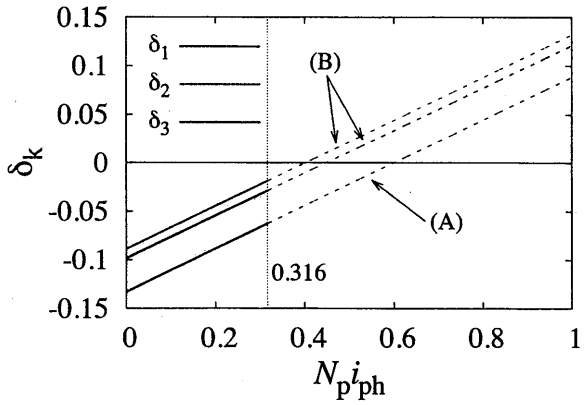

Fig. 6 Change of the values of the phase angles δ_k under equilibriums: (A) uniform load profile and (B) non-uniform load profile. The *solid* lines represent the *stable* equilibriums, and the *dashed* lines the *unstable* equilibriums. The values of δ_k monotonically increase as the photoelectric current $N_{\text{p}}i_{\text{ph}}$ increases. At $N_{\text{p}}i_{\text{ph}} = 0.316$, the stability of the equilibriums changes.

3.1 Steady States

First, we consider steady-state characteristics of the three homes. Fig. 6 shows the values of phase angles δ_k under equilibriums with the change of the photoelectric current $N_{\text{p}}i_{\text{ph}}$. We consider the two cases of uniform and non-uniform load profiles: (A) $(p_{\text{load},1}, p_{\text{load},2}, p_{\text{load},3}) = (0.5, 0.5, 0.5)$ and (B) $(p_{\text{load},1}, p_{\text{load},2}, p_{\text{load},3}) = (0, 0.5, 0.5)$. We also consider the uniform photoelectric current for every home, that is, $i_{\text{ph},k} = i_{\text{ph}}$. This uniform setting of i_{ph} is valid if the three homes are geographically close. The non-uniform profile (B) results in non-uniform equilibrium values of δ_k as shown in Fig. 6. In this figure, the *solid* lines represent the *stable* equilibriums, and the *dashed* lines the *unstable* equilibriums. Thus we see that the stability of the equilibriums changes at $N_{\text{p}}i_{\text{ph}} = 0.316$. Based on the linearized system of (14) around the equilibriums, the change of stability is due to supercritical Hopf bifurcation [11] as shown in Fig. 7. After the bifurcation value, a stable limit cycle is generated around the equilibriums. The stable limit cycle implies a undamped, sustained oscillation in frequency and active power, and it is regarded as a undesirable operating condition of the power system.

3.2 Long-term Dynamics

Finally, we discuss long-term dynamics caused by a combination of the bifurcation phenomenon and uncertain change of the photoelectric current. As mentioned above, the parameter $N_{\text{p}}i_{\text{ph}}$ is uncertain and can be modeled in a probabilistic way. One example of such time series of $N_{\text{p}}i_{\text{ph}}$ is shown in the

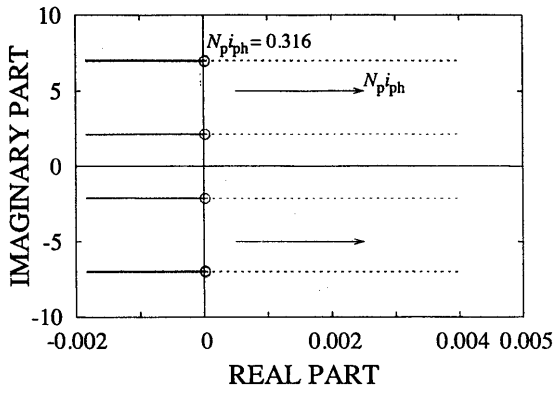

Fig. 7 Change of eigenvalues of the linearized system of (14) around equilibriums [8]. This is the case of uniform load profile (A). The change of stability of the equilibriums at $N_p i_{ph} = 0.316$, denoted by ∘, is due to supercritical Hopf bifurcation.

upper figure of Fig. 8. The value of $N_p i_{ph}$ changes at every 5 seconds. The time series is generated as a Gaussian distribution with mean 0.25 and standard deviation 0.071 [12]. The lower figure shows the probability density of the time series. The density is computed by counting the time spent for each $N_p i_{ph}$ and dividing it by the total time duration in Fig. 8. This time series is regarded as an uncertain input to the dynamical system (14). This viewpoint of the dynamical system comes from the idea of uncertainty propagation in nonlinear systems [13]. Fig. 9 shows the long-term responses of the active power output p_k against the time series of $N_p i_{ph}$. This is the case of non-uniform load profile (B). The probability densities of the active power output are also shown. We see intermittent behaviors in the course of long-term dynamics that do not appear in the time series of $N_p i_{ph}$. They result from a combination of the Hopf bifurcation and the uncertain input. While the value of $N_p i_{ph}$ is larger than the bifurcation value, the dynamics do not settle down to any equilibrium and can grow. On the other hand, while $N_p i_{ph}$ is smaller than the bifurcation value, the dynamics tend to converge to a stable equilibrium. This data suggests a possibility of complex behaviors and instabilities due to a combination of uncertain renewables and nonlinear nominal dynamics of an electric power system.

4. Concluding Remarks

We reported an initial study on nonlinear dynamics and stability of an electric power system with three homes. Numerical simulations of the models provided a part of nonlinear dynamics of the power system with three homes: supercritical Hopf bifurcation and associated sustained oscillations. Also we illustrated a dynamical effect of uncertainty input in the PV array to the active power output of each home.

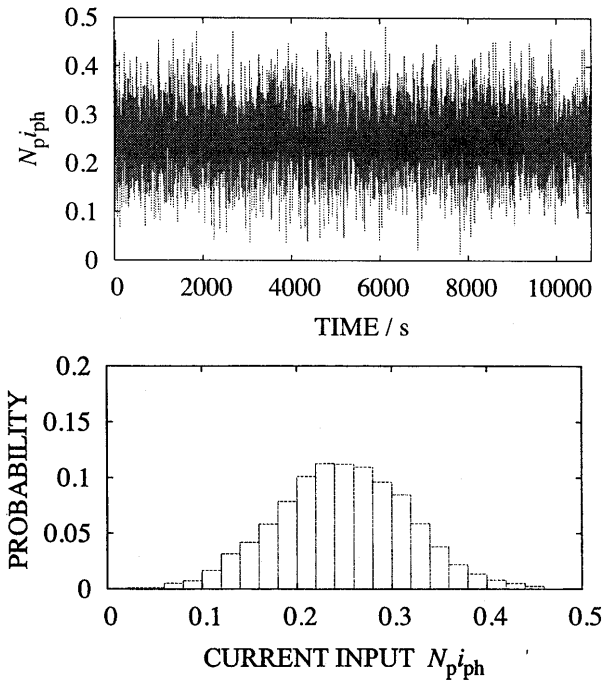

Fig. 8 One example of time series and probability density of uncertain input from the photoelectric current of the PV array. The time series is generated as a Gaussian distribution.

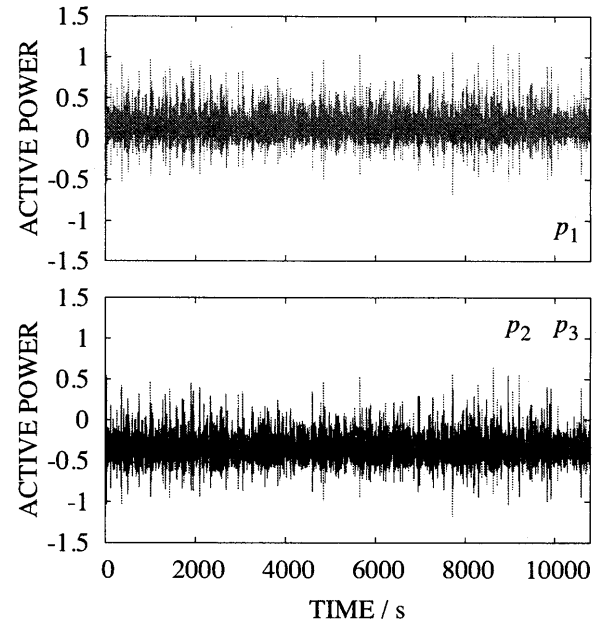

Fig. 9 Time series and probability densities of the active power output p_k while the photoelectric current $N_p i_{ph}$ changes in a probabilistic way. This is the case of non-uniform load profile (A). The intermittent dynamics are caused by a combination of the Hopf bifurcation and the random change of $N_p i_{ph}$ shown in Fig. 8.

Acknowledgement This work was supported in part by NICT Project ICE-IT.

References

[1] A. Ipakchi and F. Albuyeh, "Grid of the future," *IEEE*

Tab. 1 List of parameters of electric power system with three homes

Symbol	Meaning	Value fixed for simulation	Normalized Value
$R_{\mathrm{sh(pv)}}$	Internal shunt resistance in the PV cell model	$10\,\Omega$	0.439
I_0	Reverse bias saturation current of the PV cell model	1.0×10^{-15} A	6.17×10^{-17}
q	Elementary charge	$1.602\,176\,487(40) \times 10^{-19}$ C	
k_{B}	Boltzmann constant	$1.380\,6504(24) \times 10^{-23}$ J/K	
T	Temperature (in Kelvin)	300 K	
V_T	Thermal voltage $k_{\mathrm{B}}T/q$	0.0258 V	6.97×10^{-5}
N_{s}	Number of the PV cells connected in a series way	480	480
N_{p}	Number of the PV cells connected in a parallel way	20	20
$p_{\mathrm{load},k}$	Power consumed in the load of home #k		(in text)
δ_4	Phase angle of the commercial power grid (infinite bus)	0	0
ω_0	Nominal angular frequency	$2\pi \times 60$ Hz	1
E_0	Nominal value of the dc system voltage $e_{\mathrm{dc},k}$ in home #k	370 V	1
K	Gain constant of the Voltage-Controlled Oscillator (VCO)	1.109 rad/s/V	1
C	Smoothing capacitance in the interface circuit	10 mF	85.95
$R + \mathrm{j}X$	Line impedance between nearest neighbor homes	$3.0 \times 10^{-3}\,\Omega$ (R)	4.5×10^{-4}
		$4.0 \times 10^{-3}\,\Omega$ (X)	6.0×10^{-4}
$R_\infty + \mathrm{j}X_\infty$	Line impedance connected to the commercial power grid	$3.0 \times 10^{-2}\,\Omega$ (R_∞)	4.5×10^{-3}
		$4.0 \times 10^{-2}\,\Omega$ (X_∞)	6.0×10^{-3}
X_{T}	Transformer reactance		0.06
X_{L}	Linkage reactance between a home and the distribution network		0.02

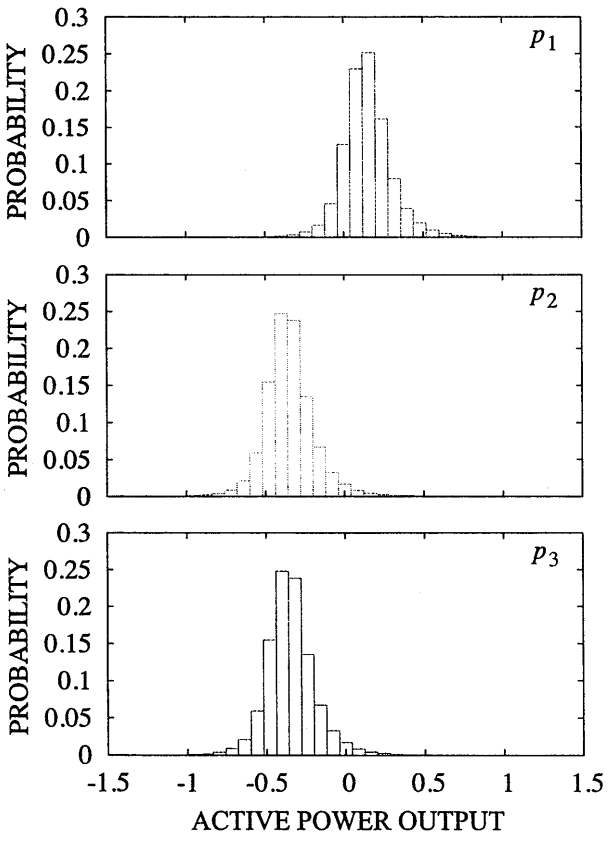

Fig. 9 (*continued*)

Power & Energy Magazine, vol. 7, no. 2, pp. 52–62, March-April 2009.

[2] "Special Features on i-Energy: Electric Power Management by Information Technologies," *IPSJ Magazine*, vol. 51, no. 8, pp. 924–985, August 2010, (in Japanese).

[3] "Special Issue on Recent Development of Energy Systems Technologies—Monitoring Energy Consumption with ICT and its Applications," *Systems, Control, and Information*, vol. 55, no. 6, pp. 215–258, June 2011, (in Japanese).

[4] "Special Section on Science and Technolgy for Smart Energy Management," *Nonlinear Theory and its Applications, IEICE*, vol. 2, no. 3, pp. 262–362, July 2011.

[5] K. Harada and K. Murata, "Interface circuit between solar-cell and commercial ac bus," *Transactions of the Institute for Engineers of Communications and Electronics*, vol. J69-C, no. 11, pp. 1458–1464, November 1986, (in Japanese).

[6] ——, "On the automatic interconnection between solar cell and ac power source," in *Proceedings of the Telecommunications Energy Conference*, New Orleans, USA, November 1984, pp. 259–262.

[7] T. Hikihara, T. Sawada, and T. Funaki, "Enhanced entrainment of synchronous inverters for distributed power sources," *IEICE Trans. Fund. Electr.*, vol. E90-A, no. 11, pp. 2516–2525, November 2007.

[8] Y. Susuki, R. Kazaoka, and T. Hikihara, "Design of electric power system with multiple homes (1,2)," in *Proc. 55th Annual Conference of the Institutes of Systems, Control and Information Engineers (ISCIE)*, Osaka, Japan, May 2011, pp. 55–58, (in Japanese).

[9] ——, "Physical architectures and mathematical models for electric-power management of multiple homes," in *50th IEEE Conference on Decision and Control and European Control Conference*, December 2011, (to appear).

[10] P. Kundur, *Power System Stability and Control*. McGraw-Hill, 1994.

[11] J. Guckenheimer and P. Holmes, *Nonlinear Oscillations, Dynamical Systems, and Bifurcations of Vector Fields*, ser. Applied Mathematical Sciences. New York: Springer-Verlag, 1983, vol. 42.

[12] K. J. Åström, *Introduction to Stochastic Control Theory*. New York: Dover Publications, 2006.

[13] I. Mezić and T. Runolfsson, "Uncertainty propagation in dynamical systems," *Automatica*, vol. 44, pp. 3003–3013, November 2006.